

Article

Bio-Mitigation of Carbon Dioxide Using *Desmodesmus* sp. in the Custom-Designed Pilot-Scale Loop Photobioreactor

Abhishek Anand ¹, Kaustubh Tripathi ¹, Amit Kumar ¹, Suresh Gupta ¹, Smita Raghuvanshi ^{1,*} and Sanjay Kumar Verma ²

¹ Department of Chemical Engineering, Birla Institute of Technology and Science (BITS), Pilani 333031, Rajasthan, India; p20170014@pilani.bits-pilani.ac.in (A.A.); f2014538@pilani.bits-pilani.ac.in (K.T.); h20170029@pilani.bits-pilani.ac.in (A.K.); sureshg@pilani.bits-pilani.ac.in (S.G.)

² Department of Biological Sciences, Birla Institute of Technology and Science (BITS), Pilani 333031, Rajasthan, India; skverma@pilani.bits-pilani.ac.in

* Correspondence: smita@pilani.bits-pilani.ac.in; Tel.: +91-1596-255638

Abstract: Today's society is faced with many upfront challenges such as the energy crisis, water pollution, air pollution, and global warming. The greenhouse gases (GHGs) responsible for global warming include carbon dioxide (CO₂), methane (CH₄), nitrous oxide (NO_x), water vapor (H₂O), and fluorinated gases. A fraction of the increased emissions of CO₂ in the atmosphere is due to agricultural and municipal solid waste (MSW) management systems. There is a need for a sustainable solution which can degrade the pollutants and provide a technology-based solution. Hence, the present work deals with the custom design of a loop photobioreactor with 34 L of total volume used to handle different inlet CO₂ concentrations (0.03%, 5%, and 10% (v/v)). The obtained values of biomass productivity and CO₂ fixation rate include $0.185 \pm 0.004 \text{ g L}^{-1} \text{ d}^{-1}$ and $0.333 \pm 0.004 \text{ g L}^{-1} \text{ d}^{-1}$, respectively, at 10% (v/v) CO₂ concentration and $0.084 \pm 0.003 \text{ g L}^{-1} \text{ d}^{-1}$ and $0.155 \pm 0.003 \text{ g L}^{-1} \text{ d}^{-1}$, respectively, at 5% (v/v) CO₂ concentration. The biochemical compositions, such as carbohydrate, proteins, and lipid content, were estimated in the algal biomass produced from CO₂ mitigation studies. The maximum carbohydrate, proteins, and lipid content were obtained as $20.7 \pm 2.4\%$, $32.2 \pm 2.5\%$, and $42 \pm 1.0\%$, respectively, at 10% (v/v) CO₂ concentration. Chlorophyll (Chl) a and b were determined in algal biomass as an algal physiological response. The results obtained in the present study are compared with the previous studies reported in the literature, which indicated the feasibility of the scale-up of the process for the source reduction of CO₂ generated from waste management systems without significant change in productivity. The present work emphasizes the cross-disciplinary approach for the development of bio-mitigation of CO₂ in the loop photobioreactor.

Keywords: *Desmodesmus* sp.; loop photobioreactor; biomass productivity; CO₂ fixation rate; lipid



Citation: Anand, A.; Tripathi, K.; Kumar, A.; Gupta, S.; Raghuvanshi, S.; Verma, S.K. Bio-Mitigation of Carbon Dioxide Using *Desmodesmus* sp. in the Custom-Designed Pilot-Scale Loop Photobioreactor. *Sustainability* **2021**, *13*, 9882. <https://doi.org/10.3390/su13179882>

Academic Editor: Farooq Sher

Received: 9 June 2021

Accepted: 27 August 2021

Published: 2 September 2021

Publisher's Note: MDPI stays neutral with regard to jurisdictional claims in published maps and institutional affiliations.



Copyright: © 2021 by the authors. Licensee MDPI, Basel, Switzerland. This article is an open access article distributed under the terms and conditions of the Creative Commons Attribution (CC BY) license (<https://creativecommons.org/licenses/by/4.0/>).

1. Introduction

Global warming caused by rising carbon dioxide (CO₂) emissions is currently a worldwide concern. Since industrialization, global greenhouse gas (GHG) emissions have increased due to human activities [1]. The primary source of CO₂ emissions includes anthropogenic waste, fossil fuel combustion, transportation, municipal waste, and agriculture waste [2,3]. Most GHG emissions generated from agricultural waste occur through the various waste management stages and agricultural inputs, mainly from water, fertilizers, pesticides from the soil, residue management, and irrigation [4]. Another sector, municipal solid waste management, significantly contributes to GHG emissions, mainly CO₂, methane (CH₄), and nitrous oxide (N₂O). From collection to treatment and disposal, the waste management process must be optimized to reduce greenhouse gas emissions [5]. One of the previous reports suggested that the anthropogenic emission of CO₂ from municipal waste and the agriculture sector is responsible for global CO₂ emissions up to 3.2% and

18.4%, respectively [6]. According to one of the recent reports, GHG emissions from the agricultural sector, including livestock such as cows, agricultural soils, and rice production, accounted for 10% of the total GHG emissions [7].

Thus, GHG emissions from municipal solid waste and agriculture waste treatment methods have raised concerns about climate change [8,9]. CO₂ is one of the most significant GHG emissions. The estimated emission of CO₂ in 2014 was 6870 MMT (million metric tons), which contributes to around 81% of the total GHG emissions in the world [10]. Currently, CO₂ concentration is above 400 ppm (parts per million) according to the data obtained from the NOAA Earth System Research Laboratory, Global Monitoring Division [11]. The projected concentration of CO₂ will rise to the value of 600 ppm, resulting in the rise of sea level from 0.4 to 1 m. It can also lead to ocean acidification in the twenty-first century [12,13]. The Intergovernmental Panel on Climate Change (IPCC) stated that if the appropriate action is not taken to prevent the continual increase of GHG emissions, the earth's temperature will increase by 1.4–5.8 °C during the 21st century [14,15]. Hence, carbon capture sequestration (CCS) and carbon capture utilization (CCU) strategies are utilized to cut down the CO₂ emissions from sources [16,17]. The present research is emphasized in the domain of CCU [18].

The physical and chemical methods to mitigate CO₂ emissions include absorption, cryogenic separation, ionic liquids, and CO₂ storage [19,20]. However, these approaches entail higher energy consumption, construction, and operating costs [21,22]. In recent times, biological methods of CO₂ mitigation gained the attention of researchers due to the production of biomass energy during CO₂ fixation by photosynthetic processes [23,24]. Photosynthetic microorganisms such as microalgae have an efficiency of 10–50 times higher than terrestrial plants, with a CO₂ fixation rate between 0.73 and 2.22 g L⁻¹ day⁻¹ [25,26]. The microalgae-based mitigation process has several advantages, such as a higher growth rate than terrestrial plants [27] and completes the recycling of CO₂. CO₂ is converted into biomass via photosynthesis activity by utilizing nitrogen and phosphorous as a nutrient source and solar energy as an energy source, which can be further transformed into fuels using existing technologies. Later, fuels can be utilized to produce power and result in CO₂ formation [28,29].

Conventionally, algae can be cultivated in an open culture system (raceway ponds) or a closed system (photobioreactors). A study carried out on 1 L glass made in a closed photobioreactor for the bio-mitigation of CO₂ by *Scenedesmus obliquus* reported the CO₂ consumption rate values as 390.2 mg L⁻¹d⁻¹ [30]. Another study discussed the CO₂ fixation by *Scenedesmus* sp. in a closed photobioreactor having dimensions of 33 cm length and 4.5 cm inner diameter [31]. The study demonstrated an integrated system for CO₂ fixation from flue gas, wastewater remediation, and biomass production. Similarly, few studies have reported the CO₂ mitigation study on raceway pond (open pond) systems. Raceway ponds are utilized for CO₂ mitigation for the large-scale cultivation of algae species such as *Chlorella*, *Dunaliella*, and *S. platensis*, [30,32]. The raceway ponds are the best examples of open pond systems due to better nutrient mixing and biomass sedimentation. The disadvantages of raceway ponds are that, compared to the closed photobioreactor, raceway ponds show lower productivity because of the carbon limitation [32].

Closed photobioreactors mostly give higher biomass productivities and also prevent outside contamination [33]. Given the benefits of closed systems over open ponds, various photobioreactors (from laboratory to industrial scale) have been developed. Even though many photobioreactors have been studied, only a small number of these reactors can efficiently use solar energy for mass algal production. The majority of outdoor photobioreactors, such as flat-plate, horizontal, and inclined tubular photobioreactors, have exposed lightning surfaces. Bubble-column, airlift, and stirred-tank photobioreactors offer high scalability, but their application in outdoor cultures is limited due to their low illumination surface areas [33,34]. While many photobioreactors appear simple to run at the laboratory scale, only a few photobioreactors have been successfully scaled up at the pilot scale. The difficulties in maintaining optimal light, temperature, mixing, and mass transfer in photo-

bioreactors make these scale-up techniques extremely difficult. The absence of effective photobioreactors is one of the primary blockades to mass algae production.

Overcoming these limitations, loop bioreactors are efficient reactors that provide uniform and good mixing without mechanical agitation and ease of operation. These are mainly constructed of transparent materials such as glass, plexiglass, polyvinylchloride (PVC), acrylic PVC, or polyethylene [35,36]. Loop reactors are cylindrical vessels that perform the mixing of multiphase fluids without the impeller action. The advantages of the loop reactor are better mixing without impellers and an adequate illumination surface, which allow these reactors to overcome the limitations of flat-plate, horizontal, and inclined tubular photobioreactors. Another significant advantage is that the cost of impellers is not incurred in these loop reactors, leading to energy savings [37,38]. The literature studies indicated that the application of loop bioreactors for CO₂ mitigation using microalgae is limited. Most of the studies are confined to bench-scale reactors. Hence, there is an enormous scope to utilize the pilot-scale closed-loop photobioreactor for CO₂ fixation using microalgae.

The present study focuses on the bio-mitigation of CO₂ in the atmosphere by *Desmodesmus* species in the closed-loop photobioreactor (custom design) of a scale of around 34 L, which is almost a pilot-scale reactor. Bio-mitigation experiments using *Desmodesmus* species were carried out at three different CO₂ concentrations, including 0.03% (atmospheric CO₂), 5%, and 10% (v/v) in the loop photobioreactor. The work includes estimating growth kinetic parameters such as cell concentration, specific growth rate, biomass productivity, and CO₂ fixation rate. The biochemical properties, such as chlorophyll content, lipid content, carbohydrate content, protein, and cells, were determined for the obtained biomass. Thus, an optimized process was developed to effectively utilize CO₂ generated from waste and in actual day-to-day conditions. This is an economical and alternative source of carbon for the simultaneous production of biomass feedstock rich in lipids and carbohydrates in a “waste to wealth” chain and waste management for sustainable future development.

2. Materials and Methods

2.1. Media Preparation, Microalgae Strain, Culture Conditions, and Inoculum Preparation

BG-11 Medium was used as cultivation media for the growth of algae, which contains 0.04 g L⁻¹ dipotassium hydrogen phosphate (K₂HPO₄), 0.006 g L⁻¹ of citric acid (C₆H₈O₇), 0.006 g L⁻¹ of ferric ammonium citrate (C₆H_{5+4y}FE_xNyO₇), 0.001 g L⁻¹ EDTA, 1.5 g L⁻¹ of sodium nitrate (NaNO₃), 0.075 g L⁻¹ of magnesium sulfate (MgSO₄·7H₂O), 0.036 g L⁻¹ of calcium chloride (CaCl₂), 0.002 g L⁻¹ of sodium carbonate (Na₂CO₃), and 1 mL L⁻¹ of trace metal mix. Trace metal mix comprised boric acid, zinc sulfate, copper sulfate, sodium molybdate, cobalt nitrate, and manganese chloride. The solid media was used for plating and was prepared by adding 1.5 g L⁻¹ (1.5%) agar to aqueous media. The conditioned media was autoclaved at 121 °C and 15 psi for 15 min and was used for further studies.

Microalgae strain *Desmodesmus* sp. MCC34 [KF731760.1] was used in the present work [39]. It was collected from the Environment and Microbiology lab of BITS Pilani, Pilani Campus, Rajasthan. The strain was isolated from the local water bodies of Pilani, Rajasthan, as reported by Nagappan and Verma [35].

The inoculum was grown at a constant temperature of 26 ± 1 °C in the laboratory and the light intensity of 67 μmol photon m⁻² s⁻¹ for ten days. The purity of the grown culture was checked using repeated streaking of the culture on BG-11 plates. The cultures with an optical density close to unity were used as inoculum for conducting the experiments in a custom-designed loop photobioreactor at larger volumes. The optical density of culture was measured at a wavelength of 650 nm (OD) at [OD_{650 nm}] (Evolution 201, Thermo Scientific, is Waltham, MA USA) to determine the cell concentration using a UV-Vis spectrophotometer. The calibration curve was prepared between the dry weight of biomass versus optical density to measure the cell concentration.

2.2. Experimental Setup

The schematic of loop photobioreactor with detailed custom design of experimental setup is given in Figure 1.

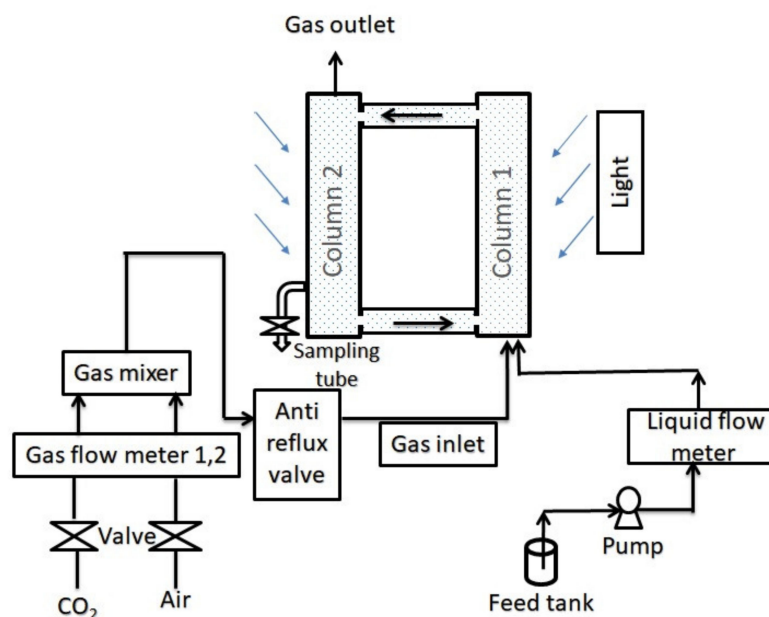


Figure 1. Schematic diagram of custom-designed loop photobioreactor.

The loop photobioreactor was constructed with two units and dimensions of 2.03 m, including 0.105 m diameter and 0.12 m outer diameter. The loop photobioreactor with a total volume of 34 L and a working volume of 26 L was designed for the overall process, and a photograph of the actual setup is given in Figure 2. The sunlight was used as the energy source during the process. In this study, 1.25 L of enriched culture was used as inoculum volume, and it had an optical density (OD) of 0.82. The experiments were performed in the semicontinuous mode.

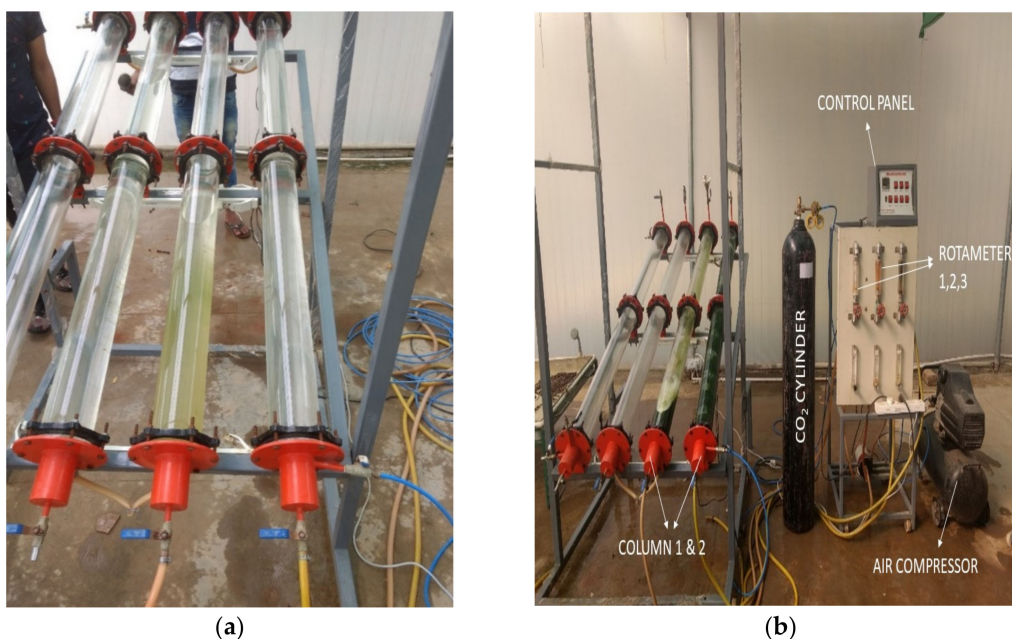


Figure 2. An overview of the loop photobioreactor: (a) at day zero after inoculation; (b) at day 12—last day of incubation period used for the CO₂ mitigation study.

2.3. Experimental Procedure

A gas mixture comprising of 10% (*v/v*) CO₂ (g) and 90% of compressed moisture-free air was utilized as a source of CO₂ (g) in the photobioreactor. The gas mixture was supplied on a 12 h aeration cycle through the gas inlet port of the photobioreactor equipped with the sparger. The gas mixture was fed during the light period, and its supply was stopped during the dark period. The continuous study was performed in a loop photobioreactor for 12 days, and the temperature was maintained at ambient conditions of 30–35 °C. The initial pH was maintained between 7 and 9 for the optimal growth of *Desmodesmus* sp. that increased the solubility of CO₂ in the aqueous phase. The flow rate of gas into the reactor was maintained at 32 vvm (4 L min⁻¹).

Once the microalgae reached the stationary phase, culture was separated by filtering with muslin cloth and was rinsed with distilled water. The algal biomass was freeze-dried and preserved at -20 °C for carrying out further studies. The parameters such as pH, dry weight biomass, and CFU were measured after every 24 h duration. The optical density (OD_{650nm}) was measured twice a day (after completion of the light cycle and a dark process). The control run was performed using ambient air (0.03% CO₂) while keeping other conditions the same. The change in color of columns 1 and 2 in picture (b) concerning picture (a) shows *Desmodesmus* sp. after 12 days of the incubation period.

2.4. Measurement of Biomass Growth Rate

The dry weight biomass and optical density were measured to evaluate the biomass yield of *Desmodesmus* sp. Fifty milliliters of aliquot culture was collected, and dry weight biomass (g L⁻¹) was measured using the standard filtration process [40,41]. The filtrate obtained was utilized for further studies. The contamination was checked by plating the supernatant and colony-forming unit (CFU) method. Aliquots were withdrawn from the loop photobioreactor every 24 h, and pH was measured using a digital pH meter (Eco Testr pH 2, Eutech Instruments).

2.5. Determination of Growth Kinetic Parameters

The biomass productivity (*P*) was calculated by the given Equation (1):

$$P = \frac{X_t - X_0}{t_t - t_0} \quad (1)$$

where X_t is the cell concentration (g L⁻¹) at the end of the cultivation cycle (t_t), and X_0 is the initial cell concentration (g L⁻¹) at t_0 (day). The specific growth rate μ_{max} (day⁻¹) was calculated using Equation (2) [42,43].

$$\mu_{max} = \frac{\ln N_2 - \ln N_1}{t_2 - t_1} \quad (2)$$

where N_1 and N_2 are the concentrations of the cells at the beginning (t_1) and the end (t_2) of the exponential growth phase, respectively [43,44]. C₁O_{0.48} H_{1.83}N_{0.11}P_{0.01} was used as the microalgal biomass molecular formula stated in previous studies [45]. As per the reported studies, it is assumed that 1 g of produced algal biomass (C₁O_{0.48} H_{1.83}N_{0.11}P_{0.01}) is equivalent to capture 1.88 g of CO₂, and hence, the CO₂ fixation rate (g L⁻¹ d⁻¹) was determined from Equation (3) [31,46].

$$\text{Fixation rate of CO}_2 = 1.88 \times P_{\text{overall}} \quad (3)$$

where P_{overall} is the overall biomass productivity. CO₂ utilization efficiency was obtained from Equation (4).

$$\text{CO}_2 \text{ utilization efficiency} = \frac{\text{fixation rate of CO}_2}{\text{CO}_{2in}} \times 100 \quad (4)$$

2.6. Determination of Chlorophyll Content

Fifty milliliters of algal culture sample was collected in the falcon tube and was centrifuged for 10 min at 4000 rpm. The supernatant was discarded, and the pellet was stored at $-20\text{ }^{\circ}\text{C}$ until further use. During the extraction step, the pellet was re-suspended in 90% methanol. It was further assisted by sonication for cell lysis under dark conditions in the ice bath (to prevent the degradation of chlorophyll from light). The control parameters followed during the sonication were of 1 min timer and a 60% duty cycle. The thermal shock was given by the snap freezing method in liquid nitrogen, and the whole process was repeated for ten cycles to maximize the extraction yield. This step was followed by centrifugation at 4000 rpm for 10 min, and the pellet was dried and stored. One milligram of dried algal biomass was taken in the falcon tube, and a mixture of 90% methanol and 10% Millipore water was added to maintain the volume of 10 mL. The tube was kept in the water bath for 20 min, and then it was stored at $4\text{ }^{\circ}\text{C}$ for the incubation period of 24 h. The absorbance of the obtained supernatant was measured at 652 and 665 nm in a spectrophotometer. Methanol was used as a blank solution in a UV-Vis spectrophotometer. The concentration of Chl a and Chl b was determined according to the following Equations (5) and (6) [46].

$$\text{Chl a (mgL}^{-1}\text{)} = (16.72 \times \text{absorbance}_{665\text{nm}}) - (9.16 \times \text{absorbance}_{652\text{nm}}) \quad (5)$$

$$\text{Chl b (mgL}^{-1}\text{)} = (34.09 \times \text{absorbance}_{652\text{nm}}) - (15.28 \times \text{absorbance}_{665\text{nm}}) \quad (6)$$

2.7. Biochemical Compositional Analysis

Biomass collected after every sampling point (as explained in Section 2.4) has been utilized for biochemical compositional analysis.

2.7.1. Analysis of Total Carbohydrate (CHO) Content

A 5 mL sample was taken and centrifuged at $5\text{ }^{\circ}\text{C}$ for 10 min at 4000 rpm, and the obtained supernatant was discarded. The pellets were washed with deionized water and stored at $-20\text{ }^{\circ}\text{C}$ for further studies. Then, 0.5 mL of 2.5 M H_2SO_4 was added in the pellet to carry out primary hydrolysis (polysaccharides to monosaccharides) [47,48]. The samples were placed for incubation in a boiling water bath for two hours. The columns were cooled at room temperature, and hydrolysate was diluted with deionized water to make it to the volume of 5 mL. The particular step was followed by centrifugation at 4000 rpm, and the supernatant was collected. The phenol-sulfuric method was applied to determine the total content of carbohydrates in biomass [49]. The calibration plot was drawn at different glucose concentrations ($0\text{--}0.1\text{ mg mL}^{-1}$). Two-milliliter aliquots of diluted supernatant along with standard solution were mixed with 1 mL of 5% aqueous phenol in a 15 mL falcon tube. Then, 5 mL of concentrated sulfuric acid was immediately added in all tubes and then vortexed for 10 s. All falcon tubes were kept at room temperature for 10 min, and then these were placed in the water bath at $30\text{ }^{\circ}\text{C}$ to develop a yellow-golden color. The value of absorbance was measured at 490 nm in a UV-Vis spectrophotometer [50].

2.7.2. Analysis of Total Protein Content

The Folin–Lowry method was used for the total protein determination using white pellets obtained after pigment extraction [51]. The pellet was pretreated with 1% SDS/0.1 M NaOH in 500 μL . The re-suspended pellet mixed with reagent A (500 μL of 1:1:1:1 ratio of CTC (0.1% $\text{CuSO}_4 \cdot 5\text{H}_2\text{O}$ + 0.2% NaK tartrate +10% Na_2CO_3), 10% SDS, 0.8 M NaOH and dH_2O) and the tubes were kept at room temperature for 10 min. After adding reagent B (250 μL of a solution of one volume of Folin–Ciocalteu reagent and five volumes of dH_2O) to the samples, tubes were instantly vortexed and allowed to stand at room temperature for 30 min. The OD was measured at 750 nm for 0.5 mL of 1% SDS/0.1 M NaOH. The standard curve was prepared for the determination of the total amount of protein by

dissolving different concentrations of bovine serum albumin (BSA) in 1% SDS/0.1 M NaOH (0–1.0 mg mL⁻¹) as reported by Varshney et al. (2016) [52].

2.7.3. Analysis of Total Lipid Content

The total lipid content of the biomass was quantified gravimetrically using the Bligh and Dyer method with slight modifications [53]. The pellets were separated from the 50 mL culture after centrifugation at 4000 rpm for 10 min at 4 °C and were stored at –20 °C for further studies. The pellet was suspended in 2.4 mL deionized water followed by 3 mL chloroform and 6 mL methanol. It was followed by sonication by placing the mixture in the ultrasonic bath for 20 min. Further, 3 mL of each deionized water and chloroform were added to maintain the final ratio of 2:2:1.8. The final mixture was centrifuged for 10 min at 2000 rpm. The organic bottom layer of chloroform was carefully extracted after centrifugation and was transferred into a pre-weighted vial and preserved overnight for solvent evaporation in the fume hood. The vial was reweighted until dry to determine the overall lipid quantity, and these steps were carried out at room temperature as per the procedure reported by Varshney et al. (2018) [50].

3. Results and Discussion

The semicontinuous studies analyzed the growth performance of *Desmodesmus* sp. for 12 days, for the three different CO₂ concentrations, 0.03%, 5%, and 10% (v/v), in a loop photobioreactor. The obtained results from these studies were analyzed and summarized in the following sections.

3.1. Effect of CO₂ Concentration on Biomass Growth Rate and Optical Density Values

Desmodesmus sp. growth performance in the presence of different CO₂ (0.03%, 5%, and 10% v/v) concentrations was examined in a loop photobioreactor. During all experiments, microalgae showed a short lag phase of 1 to 3 days, which indicated the suitability of gaseous CO₂ mitigation by *Desmodesmus* sp. as a carbon source, as shown in Figure 3. The trend shows the increased growth in the exponential phase for ten days at different concentrations of CO₂ due to the presence of the appropriate amount of nutrient for cell growth in the reactor.

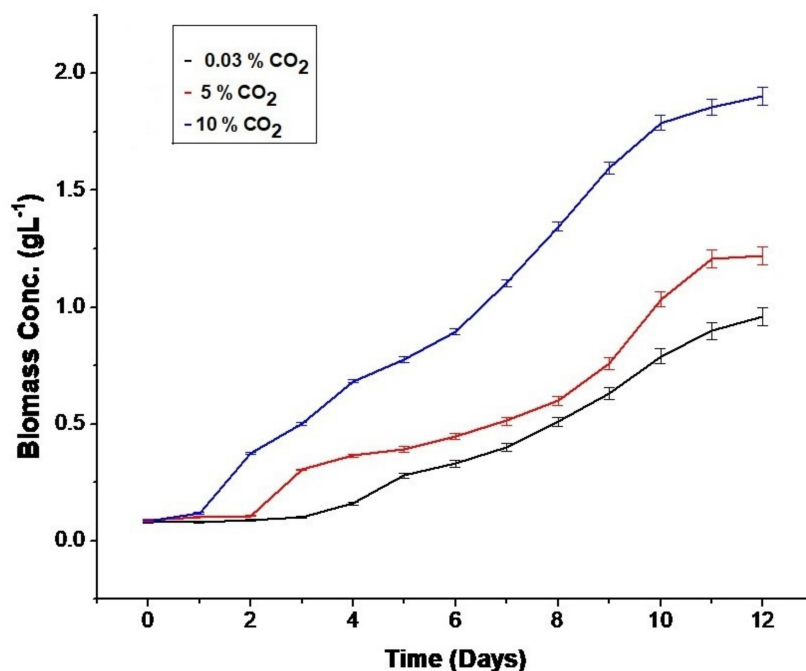


Figure 3. Effect of time on cell concentration (g L⁻¹) at three different CO₂ concentrations (0.03%, 5%, and 10% v/v).

After 12 days of incubation, culture supplemented with 10% (*v/v*) CO₂ showed $1.903 \pm 0.038 \text{ g L}^{-1}$ of cell concentration on a dry cell weight (DCW) basis, which is higher as compared to the culture grown at 0.03% of CO₂ *v/v* ($0.96 \pm 0.039 \text{ g L}^{-1}$) and at 5% CO₂ *v/v* ($1.219 \pm 0.040 \text{ g L}^{-1}$). The cell concentration in cultures supplied with 5% CO₂ and 10% CO₂ was higher than the cultures with ambient air conditions, suggesting that CO₂ as a carbon source facilitated microalgae growth [54,55]. A similar trend was reported for CO₂ mitigation in earlier reported studies [56,57].

The results are also plotted to understand the light and dark cycle (L/D cycle) on biomass growth rate in optical density (OD_{650nm}) at three different CO₂ concentrations and are given in Figure 4. The values of optical density were measured twice a day [58].

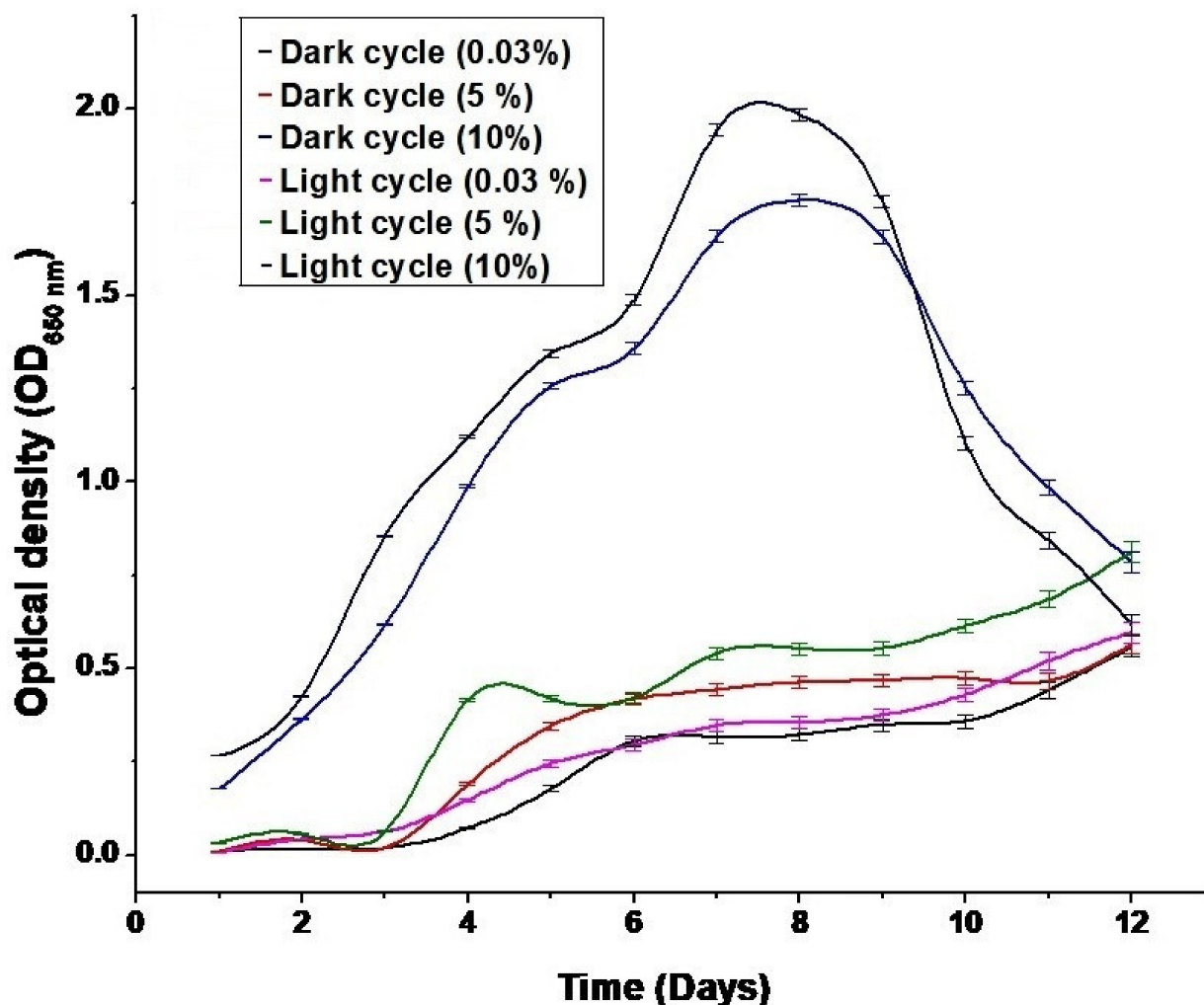


Figure 4. Effect of light and dark cycle on optical density (OD) with respect to time for three different CO₂ concentrations.

The maximum OD values were obtained during the light cycle as 0.60 ± 0.017 , 0.81 ± 0.016 , and 1.99 ± 0.010 and during the dark cycle as 0.56 ± 0.016 , 0.57 ± 0.017 , and 1.76 ± 0.009 at 0.03% CO₂, 5% CO₂, and 10% CO₂ concentrations, respectively. The increased absorbance values during the light cycle compared to the dark cycle confirmed that the photosynthesis process is enhanced during the day and microalgal growth is better during the light period. The increase in the biomass concentration values during the day cycle enhances the understanding that the increased biomass concentration is due to the increased cell growth, and hence is greatly dependent on the sunlight intensity [59].

It has been reported by the researchers that the photosynthetic efficiency of microalgae under intermittent illumination is known to be higher than under continuous illumination, provided that the parameters of the L/D cycle are tuned correctly [60,61]. The reasoning could be that photosynthesis is a cyclic process, where a slower thermochemical process follows almost instantaneous photochemical reactions.

3.2. Effects of CO₂ Concentration on Growth Kinetic Parameters

3.2.1. Specific Growth Rate

The specific growth rate (μ) of algal culture was measured using Equation (2) as given in Section 2.5. The maximum value of μ_m was obtained as $0.15 \pm 0.004 \text{ d}^{-1}$ when algal cells were grown with 10% inlet CO₂ concentration. The specific growth rate was observed to be $0.07 \pm 0.002 \text{ d}^{-1}$ and $0.13 \pm 0.003 \text{ d}^{-1}$ for 0.03% and 5% inlet CO₂ concentration, respectively (Figure 5). The marginal difference in the value of μ was observed to change CO₂ concentration from 5% to 10%. These results are as per the reported results in the earlier studies [57,62].

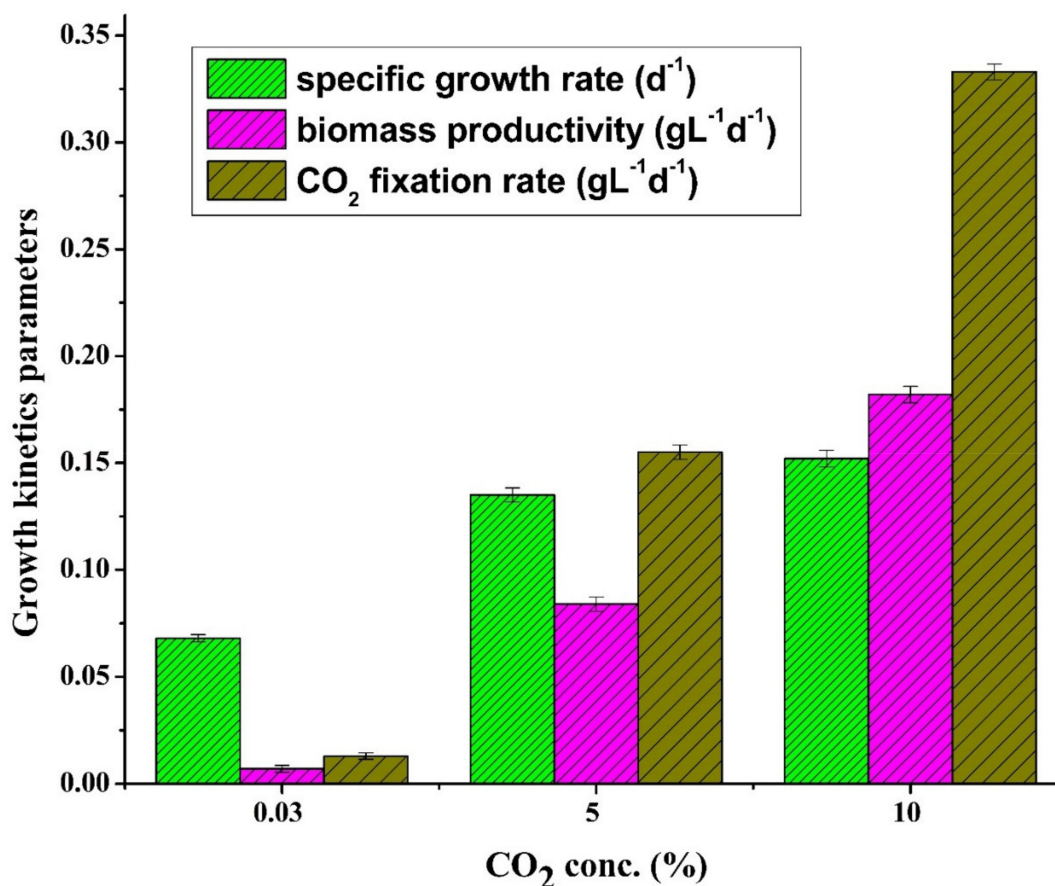


Figure 5. Effect of three different CO₂ concentrations (0.03%, 5%, and 10% v/v) on the different growth kinetic parameters (specific growth rate (d⁻¹), biomass productivity (g L⁻¹ d⁻¹), CO₂ fixation rate (g L⁻¹ d⁻¹)) of microalgae.

3.2.2. Biomass Productivity

The concentration of CO₂ significantly influences the productivity of biomass. The biomass productivity was estimated for all three inlet concentrations and is shown in Figure 5. It was observed that with the increase in CO₂ concentration from 0.03% to 10%, the biomass productivity value was increased from $0.018 \pm 0.002 \text{ g L}^{-1} \text{ d}^{-1}$ to $0.185 \pm 0.004 \text{ g L}^{-1} \text{ d}^{-1}$. These findings are consistent with values obtained by studies given by [45,62].

3.2.3. CO₂ Fixation Rate

The CO₂ fixation rate was calculated using Equation (3). It was observed that the higher rate of biofixation of CO₂ ($0.33 \pm 0.004 \text{ g L}^{-1} \text{ d}^{-1}$) was achieved when microalgae were cultured at 10% inlet concentration of CO₂ (Figure 5). The CO₂ fixation rates were obtained as $0.01 \pm 0.001 \text{ g L}^{-1} \text{ d}^{-1}$ and $0.15 \pm 0.003 \text{ g L}^{-1} \text{ d}^{-1}$ for 0.03% and 5% of CO₂ concentration, respectively. These results are supported by the work carried out by different researchers [57,63].

3.3. Effect of CO₂ Concentration on Biochemical Composition of *Desmodesmus* sp.

The content of lipids, total carbohydrates, proteins, and chlorophyll was estimated as macromolecular composition in the form of percentages of the total dry biomass (DCW) at three different CO₂ concentrations (0.03%, 5%, and 10% *v/v*). The concentration of CO₂ has a significant impact on the carbohydrate (CHO) content of microalgae [52]. CHO content of microalgae was observed as $14.6 \pm 1.5\%$, $17.2 \pm 2.0\%$, and $20.7 \pm 2.4\%$ of DCW for 0.03% CO₂, 5% CO₂, and 10% CO₂ (*v/v*) concentration, respectively (Table 1). The different stages of growth and varying concentrations of CO₂ have a greater impact on the total content of carbohydrates in the harvested algal biomass. The carbohydrate content in the algal biomass was significantly increased with an increase in CO₂ concentration. The higher content of carbohydrates opens the possibility for further utilization of algal biomass as a substrate.

Table 1. Biochemical compositions of *Desmodesmus* sp. in the form of percentages of the total dry biomass (DCW) at three different CO₂ concentrations for 12 days of cultivation time.

Biochemical Composition	Inlet Concentration of CO ₂ (<i>v/v</i>)		
	0.03%	5%	10%
Total carbohydrates (% DCW)	14.6 ± 1.5	17.2 ± 2.0	20.7 ± 2.4
Proteins (% DCW)	14.4 ± 1.2	25 ± 1.1	32.3 ± 2.5
Lipids (% DCW)	15.5 ± 0.5	40 ± 2.0	42 ± 1.0
Chlorophyll a, b (mg L ⁻¹)	0.12	0.13	0.14
	0.15	0.17	0.19

The maximum protein content of $32.3 \pm 2.5\%$ DCW was obtained when algal cells were cultivated with 10% CO₂. The protein content was obtained as $14.4 \pm 1.2\%$ and $25 \pm 1.1\%$ when algal cells were grown at 0.03% and 5% CO₂, respectively (Table 1). The higher cell concentration with an increase in CO₂ concentration significantly increases the efficiency of the photosynthesis period. It leads to the formation of more and more amounts of protein.

The lipid content in algal biomass was observed to increase CO₂ concentration (Table 1). The maximum amount of lipid, about $42 \pm 1.0\%$ DCW, was accumulated at 10% CO₂. The lipid content was obtained as $15.5 \pm 0.5\%$ and $40 \pm 2.0\%$ for inlet CO₂ concentration of 0.03% and 5%, respectively. The scarcity of nitrogen and phosphorus due to their continuous utilization in microalgae cultivation may be the reason for higher lipid content [64].

The concentration of Chl a and Chl b were estimated using Equations (5) and (6), respectively, as is shown in Table 1 at different inlet CO₂ concentration of 0.03%, 5%, and 10% CO₂ (*v/v*). Chl a and Chl b concentration varies from 0.12 ± 0.001 to $0.14 \pm 0.004 \text{ mg L}^{-1}$ and 0.15 ± 0.002 to $0.19 \pm 0.005 \text{ mg L}^{-1}$ with the increase in inlet CO₂ concentration from 0.03% to 10%, respectively. The maximum amount of chlorophyll a and chlorophyll b was $0.14 \pm 0.004 \text{ mg L}^{-1}$ and $0.19 \pm 0.005 \text{ mg L}^{-1}$, respectively, when algae were treated with a 10% CO₂ concentration. It is observed that Chl a content is less than Chl b for all inlet CO₂ concentrations. It may be because the chlorophyll content in the microalgae varies in response to physical and chemical factors such as light intensity, agitation, temperature,

and nutrient availability [65,66]. In the present study, the microalgae species, *Desmodesmus*, is a genus of green algae in the family of *Scenedesmaceae*. In the green algae, chlorophyll b absorbs energy from wavelengths of green light at 640 nm, which may be a possible reason for a higher content of chlorophyll b in *Desmodesmus* sp. The concentration of chlorophyll a indicates the quantity and capacity of photosynthesis activity of microalgae. It can also be used to assess the physiological state of microalgae.

4. Performance Comparison of Loop Bioreactor

Table 2 shows the comparison of the performance of the custom-designed loop bioreactor with other reactors at different scales (bench, pilot, and large) in terms of the parameters such as biomass productivity ($\text{g L}^{-1} \text{d}^{-1}$), CO_2 fixation rate, and biochemical compositions (carbohydrate, protein, and lipid content) for CO_2 fixation via algal species. The maximum biomass produced ($1.903 \pm 0.038 \text{ g L}^{-1}$), biomass productivity ($0.19 \pm 0.004 \text{ g L}^{-1} \text{d}^{-1}$), and CO_2 fixation rate ($0.33 \pm 0.004 \text{ g L}^{-1} \text{d}^{-1}$) at 10% CO_2 concentration are higher or nearly the same as compared to the values reported for previous studies (Table 2). The carbohydrate ($20.7 \pm 2.4\%$) and protein ($32.3 \pm 2.5\%$) content obtained in the present study at 10% CO_2 concentration are comparable with the values reported for previous studies. However, the lipid content ($42 \pm 1.0\%$) is maximum compared to the studies reported in the literature. Most of the earlier studies were limited to the working volume of less than 1 L, except for a few studies. Compared to the large-scale bioreactors reported in the literature, the custom-designed loop bioreactor has shown better performance except for one study [35,67–69]. The scaled-up loop bioreactor has established comparable parameters that indicated the possibility of further scale-up of the process for the large-scale fixation of CO_2 and simultaneous algal biomass production, leading to by-product formation. This study may be a viable solution for the source reduction of CO_2 generated from waste management systems. The higher biomass productivity and carbohydrate content may lead to the value addition of the process in biofuels as by-product formation.

Table 2. Performance comparison of loop bioreactor in terms of various parameters with reported studies.

Species	Cultivation Time (Day)	Mode/ (Volume, L/Working Volume, L)	CO ₂ conc. (% v/v)	Max. Biomass Produced (X _{Max}) (g L ⁻¹)	Biomass Productivity (P) (g L ⁻¹ d ⁻¹)	CO ₂ Fixation Rate (R _{CO₂}) (g L ⁻¹ d ⁻¹)	Carbohydrate (% DCW)	Protein (% DCW)	Lipids (% DCW)	References
<i>Chlorella</i> sp.	8	Column Photobioreactors, (0.8)	2	1.21	0.15	0.28	-	-	-	Chiu et al., 2008 [67]
<i>Chlorella vulgaris</i>	15	Bio Flow fermenter, (11/8)	10	1.94	0.13	0.25	16.74	40.95	9.95	Sydney et al., 2010 [70]
<i>Scenedesmus obliquus</i>	6	Erlenmeyer flask, (0.650)	10	1.84	0.15	0.29	-	-	22	Tang et al., 2011 [45]
<i>Chlorella sorokiniana</i>	8	Airlift photobioreactor, (1.4)	4	1.1	0.15	-	-	-	20.93	Kumar et al., 2014 [71]
<i>Scenedesmus</i> sp.	7	Airlift photobioreactor, (0.5)	2.5	1.3	0.19	0.35	10.4	-	35.6	Nayak et al., 2016 [72]
<i>Scenedesmus</i> sp.	7	Bubble-column photobioreactor, (0.5)	2.5	1.37	0.196	0.37	-	-	33.3	Nayak et al., 2016 [72]
<i>Acutodesmus</i> sp.	5	Erlenmeyer flasks, (0.5/0.2)	20	1.65	-	-	34.52	38.78	11.67	Yadav et al., 2015 [55]
<i>A. quadricellulare</i>	6	Laboratory scale photobioreactor, (0.8/0.680)	5	1.29	-	-	33.4	30.3	44	Varshney et al., 2018 [53]
<i>Desmodesmus</i> sp. MCC34	18	Raceway pond, (1000)	-	1.9	-	-	-	-	0.103	Nagappan et al., 2016 [39]
<i>Porphyridium cruentum</i>	-	Airlift tubular, (200)	-	3.0	1.50	-	-	-	-	Yen et al., 2015 [71]
<i>Chlorella sorokiniana</i>	-	Inclined tubular, (6.0)	5	1.50	1.47	-	-	-	-	Ugwu et al., 2002 [69]
<i>Arthrospira platensis</i>	-	Undular row tubular, (11)	-	-	2.70	-	-	-	-	Carlozzi P., 2003 [73]
<i>Phaeodactylum tricornutum</i>	9	Outdoor helical tubular, (75)	-	2.95	1.40	-	-	-	-	Hall et al., 2003 [74]
<i>Haematococcus pluvialis</i>	16	Bubble-column, (55)	-	1.4	0.06	-	-	-	-	Lopez et al., 2006 [75]
<i>Chlorella pyrenoidosa</i>	1.25	Tubular batch reactors, (0.660)	10	-	0.11	0.096	-	-	-	Kargupta et al., 2015 [76]
<i>Chlorella</i> PY-ZU1	4.5	Cylindrical PBR (6)	15	-	0.47	0.87	-	-	-	Ye et al., 2018 [77]
<i>Desmodesmus</i> sp.	12	Loop photobioreactor, (34/26)	0.03	0.96 ± 0.04	0.018 ± 0.002	0.013 ± 0.001	14.6 ± 1.5	14.4 ± 1.2	15.5 ± 0.5	Present study
<i>Desmodesmus</i> sp.	12	Loop photobioreactor, (34/26)	5	1.219 ± 0.04	0.084 ± 0.003	0.155 ± 0.003	17.2 ± 2.0	25 ± 1.1	40 ± 2.0	Present study
<i>Desmodesmus</i> sp.	12	Loop photobioreactor, (34/26)	10	1.903 ± 0.04	0.185 ± 0.004	0.333 ± 0.004	20.7 ± 2.4	32.3 ± 2.5	42 ± 1.0	Present study

5. Conclusions

Biofixation of CO₂ (g) at three different concentrations (0.03%, 5%, and 10% *v/v*) by *Desmodesmus* sp. was successfully demonstrated in the custom-designed loop photobioreactor. The maximum values of specific growth rate, biomass productivity, and CO₂ fixation rate were obtained as 1.903 ± 0.04 g L⁻¹, 0.19 ± 0.004 g L⁻¹ d⁻¹, and 0.333 ± 0.004 g L⁻¹ d⁻¹, respectively, at 10% CO₂ concentration. The higher values of carbohydrate ($20.7 \pm 2.4\%$), protein ($32.3 \pm 2.5\%$), and lipid ($42 \pm 1.0\%$) content at 10% CO₂ concentration confirmed the suitability of *Desmodesmus* sp. for the fixation of higher CO₂ concentrations. The concentration of Chl *a* indicated the possibility of more significant photosynthesis activity of *Desmodesmus* sp. It can be concluded from the comparison of the present study with the studies reported in the literature that the use of a scaled-up loop bioreactor could possibly be utilized for large-scale fixation of CO₂ emitted from waste management sources and reduces the problem of greenhouse gas emission. The more excellent biochemical constituents in algal biomass can also be utilized as potential feedstocks for biofuel applications. Thus, the present study leads to a waste-to-wealth process as a sustainable and eco-friendly strategy for biofuel component production with CO₂ sequestration.

Author Contributions: The present research work is interdisciplinary research work. Please acknowledge: Conceptualization, S.R. and S.G.; methodology, S.R., S.G. and S.K.V.; validation, S.G.; formal analysis, S.R., S.G. and A.A.; investigation, A.A., K.T. and A.K.; data curation, A.A., K.T. and S.G.; writing—original draft preparation, A.A. and S.R.; writing—review and editing, S.R. and S.G.; visualization, S.R. and S.K.V.; supervision, S.R.; project administration, S.G. and S.K.V.; funding acquisition, S.R. and S.G. All authors have read and agreed to the published version of the manuscript.

Funding: The corresponding author would like to thank Science and Engineering Research Board—Core Research Grant, SERB—CRG, India for granting the project in the related area (CRG/2018/002943).

Institutional Review Board Statement: Not Applicable.

Informed Consent Statement: Not Applicable.

Data Availability Statement: Data is available on request from the corresponding author.

Acknowledgments: The authors are thankful to Birla Institute of Technology and Science (BITS), Pilani campus, India for providing the facilities to carry out the detailed research work.

Conflicts of Interest: The authors declare no conflict of interest. The funders had no role in the design of the study; in the collection, analyses, or interpretation of data; in the writing of the manuscript, or in the decision to publish the results.

References

1. Ramanathan, V. The greenhouse theory of climate change: A test by an inadvertent global experiment. *Science* **1988**, *240*, 293–300. [CrossRef]
2. Mendiara, T.; García-Labiano, F.; Abad, A.; Gayán, P.; de Diego, L.F.; Izquierdo, M.; Adánez, J. Negative CO₂ emissions through the use of biofuels in chemical looping technology: A review. *Appl. Energy* **2018**, *232*, 657–684. [CrossRef]
3. Sharma, J.; Kumar, S.; Kumar, V.; Malyan, S.K.; Mathimani, T.; Bishnoi, N.R.; Pugazhendhi, A. Upgrading of microalgal consortia with CO₂ from fermentation of wheat straw for the phycoremediation of domestic wastewater. *Bioresour. Technol.* **2020**, *305*, 123063. [CrossRef]
4. Agriculture, Agro-biodiversity and Climate Change. Available online: <https://www.un.org/en/ecosoc/docs/pdfs/agriculture.pdf> (accessed on 27 August 2021).
5. Calabrò, P.S. Greenhouse gases emission from municipal waste management: The role of separate collection. *Waste Manag.* **2009**, *29*, 2178–2187. [CrossRef]
6. Indian Network for Climate Change Assessment (INCCA). *India: Green House Gas Emissions 2007*; Ministry of Environment and Forests (MoEF), Government of India: New Delhi, India, 2010.
7. Sources of Greenhouse Gas Emissions. Available online: <https://www.epa.gov/ghgemissions/sources-greenhouse-gas-emissions> (accessed on 27 August 2021).
8. Chen, Y.C.; Lo, S.L. Evaluation of greenhouse gas emissions for several municipal solid waste management strategies. *J. Clean Prod.* **2016**, *113*, 606–612. [CrossRef]

9. Vetter, S.H.; Sapkota, T.; Hillier, J.; Stirling, C.M.; Macdiarmid, J.I.; Aleksandrowicz, L.; Green, R.; Joy, E.J.; Dangour, A.D.; Smith, P. Greenhouse gas emissions from agricultural food production to supply Indian diets: Implications for climate change mitigation. *Agric. Ecosyst. Environ.* **2017**, *237*, 234–241. [CrossRef] [PubMed]
10. Shahid, A.; Malik, S.; Zhu, H.; Xu, J.; Nawaz, M.Z.; Nawaz, S.; Alam, A.; Mehmood, M.A. Cultivating microalgae in wastewater for biomass production, pollutant removal, and atmospheric carbon mitigation; a review. *Sci. Total Environ.* **2020**, *704*, 135303. [CrossRef]
11. Earth System Research Laboratory, Global Monitoring, Division National Oceanic and Atmospheric Administration, U.S. Department of Commerce. The NOAA Earth System Research Laboratory, Gl. 2020. Available online: <http://www.esrl.noaa.gov/gmd/ccgg/trends> (accessed on 5 January 2020).
12. Solomon, S.; Plattner, G.K.; Knutti, R.; Friedlingstein, P. Irreversible climate change due to carbon dioxide emissions. *Proc. Natl. Acad. Sci. USA* **2009**, *106*, 1704–1709. [CrossRef]
13. Anand, A.; Raghuvanshi, S.; Gupta, S. Trends in carbon dioxide (CO₂) fixation by microbial cultivations. *Curr. Sustain. Energy Rep.* **2020**, *7*, 40–47. [CrossRef]
14. De Silva, G.P.D.; Ranjith, P.G.; Perera, M.S.A. Geochemical aspects of CO₂ sequestration in deep saline aquifers: A review. *Fuel* **2015**, *155*, 128–143. [CrossRef]
15. IPCC (Intergovernmental Panel on Climate Change). *Climate Change 2013: The Physical Science Basis*; Working Group I Contribution to the IPCC Fifth Assessment Report; Cambridge University Press: Cambridge, UK, 2013.
16. Seyed Hosseini, N.; Shang, H.; Scott, J.A. Biosequestration of industrial off-gas CO₂ for enhanced lipid productivity in open microalgae cultivation systems. *Renew Sustain. Energy Rev.* **2018**, *92*, 458–469. [CrossRef]
17. Barahoei, M.; Hatamipour, M.S.; Afsharzadeh, S. CO₂ capturing by *Chlorella vulgaris* in a bubble column photo-bioreactor; Effect of bubble size on CO₂ removal and growth rate. *J. CO₂ Util.* **2020**, *37*, 9–19. [CrossRef]
18. Khandelwal, A.; Anand, A.; Raghuvanshi, S.; Gupta, S. Integrated approach for microbial carbon dioxide (CO₂) fixation process and wastewater treatment for the production of hydrocarbons: Experimental studies. *J. Environ. Chem. Eng.* **2021**, *9*, 105116. [CrossRef]
19. Ho, S.H.; Chen, C.Y.; Lee, D.J.; Chang, J.S. Perspectives on microalgal CO₂ emission mitigation systems—A review. *Biotechnol. Adv.* **2011**, *29*, 189–198. [CrossRef] [PubMed]
20. Nocito, F.; Dibenedetto, A. Atmospheric CO₂ mitigation technologies: Carbon capture utilization and storage. *Curr. Opin. Green Sustain. Chem.* **2020**, *21*, 34–43. [CrossRef]
21. Könst, P.; Mireles, I.H.; Van Der Stel, R.; Van Os, P.; Goetheer, E. Integrated system for capturing CO₂ as feedstock for algae production. *Energy Procedia* **2017**, *114*, 7126–7132. [CrossRef]
22. Farrelly, D.J.; Everard, C.D.; Fagan, C.C.; McDonnell, K.P. Carbon sequestration and the role of biological carbon mitigation: A review. *Renew Sustain. Energy Rev.* **2013**, *21*, 712–727. [CrossRef]
23. Salbitani, G.; Barone, C.M.A.; Carfagna, S. Effect of bicarbonate on growth of the oleaginous microalga *Botryococcus braunii*. *Int. J. Plant Biol.* **2019**, *10*, 35–37. [CrossRef]
24. Mountourakis, F.; Papazi, A.; Kotzabasis, K. The microalga *Chlorella vulgaris* as a natural bioenergetic system for effective CO₂ mitigation—New perspectives against global warming. *Symmetry* **2021**, *13*, 997. [CrossRef]
25. Anguselvi, V.; Ebhin Masto, R.; Mukherjee, A.; Kumar Singh, P. CO₂ Capture for industries by algae. *Algae* **2019**, 1–11. [CrossRef]
26. Alami, A.H.; Tawalbeh, M.; Alasad, S.; Ali, M.; Alshamsi, M.; Aljaghoub, H. Cultivation of *Nannochloropsis* algae for simultaneous biomass applications and carbon dioxide capture. *Energy Sources Part A Recover. Util. Environ. Eff.* **2021**, 1–12. [CrossRef]
27. Ullmann, J.; Grimm, D. Algae and their potential for a future bioeconomy, landless food production, and the socio-economic impact of an algae industry. *Org. Agric.* **2021**, *11*, 261–267. [CrossRef]
28. Wang, B.; Li, Y.; Wu, N.; Lan, C.Q. CO₂ bio-mitigation using microalgae. *Appl. Microbiol. Biotechnol.* **2008**, *79*, 707–718. [CrossRef]
29. Leong, Y.K.; Chew, K.W.; Chen, W.H.; Chang, J.S.; Show, P.L. Reuniting the biogeochemistry of algae for a low-carbon circular bioeconomy. *Trends Plant Sci.* **2021**, *26*, 729–740. [CrossRef]
30. Ho, S.H.; Chen, C.Y.; Yeh, K.L.; Chen, W.M.; Lin, C.Y.; Chang, J.S. Characterization of photosynthetic carbon dioxide fixation ability of indigenous *Scenedesmus obliquus* isolates. *Biochem. Eng. J.* **2010**, *53*, 57–62. [CrossRef]
31. Nayak, M.; Karemore, A.; Sen, R. Sustainable valorization of flue gas CO₂ and wastewater for the production of microalgal biomass as a biofuel feedstock in closed and open reactor systems. *RSC Adv.* **2016**, *6*, 9111–91120. [CrossRef]
32. Lam, M.K.; Lee, K.T. Renewable and sustainable bioenergies production from palm oil mill effluent (POME): Win-win strategies toward better environmental protection. *Biotechnol. Adv.* **2011**, *29*, 124–141. [CrossRef] [PubMed]
33. Ugwu, C.U.; Aoyagi, H.; Uchiyama, H. Photobioreactors for mass cultivation of algae. *Bioresour. Technol.* **2008**, *99*, 4021–4028. [CrossRef]
34. Achinas, S.; Achinas, V.; Euverink, G.J.W. Microbiology and biochemistry of anaerobic digesters: A brief overview. In *Bioreactors: Sustainable Design and Industrial Applications in Mitigation of GHG Emissions*, 1st ed.; Elsevier: Amsterdam, The Netherlands, 2020; pp. 17–26. [CrossRef]
35. Kumar, K.; Dasgupta, C.N.; Nayak, B.; Lindblad, P.; Das, D. Development of suitable photobioreactors for CO₂ sequestration addressing global warming using green algae and cyanobacteria. *Bioresour. Technol.* **2011**, *102*, 4945–4953. [CrossRef] [PubMed]
36. Huang, Q.; Jiang, F.; Wang, L.; Yang, C. Design of photobioreactors for mass cultivation of photosynthetic organisms. *Engineering* **2017**, *3*, 318–329. [CrossRef]

37. Sharma, A.K.; Tripathi, K. Loop reactors—Advancing reactors realm: A review. *Reactors* **2016**.
38. Coker, A.K. Industrial and laboratory reactors—Chemical reaction hazards and process integration of reactors. *Ludwig's Appl. Process. Des. Chem. Petrochem. Plants* **2015**, 1095–1208. [[CrossRef](#)]
39. Nagappan, S.; Verma, S.K. Growth model for raceway pond cultivation of *Desmodesmus* sp. MCC34 isolated from a local water body. *Eng. Life Sci.* **2016**, *16*, 45–52. [[CrossRef](#)]
40. Abou-Shanab, R.A.I.; Ji, M.K.; Kim, H.C.; Paeng, K.J.; Jeon, B.H. Microalgal species growing on piggery wastewater as a valuable candidate for nutrient removal and biodiesel production. *J. Environ. Manag.* **2013**, *115*, 257–264. [[CrossRef](#)]
41. Sundaram, S.; Thakur, I.S. Biosurfactant production by a CO₂ sequestering *Bacillus* sp. strain ISTS2. *Bioresour. Technol.* **2015**, *188*, 247–250. [[CrossRef](#)]
42. Abreu, A.P.; Fernandes, B.; Vicente, A.A.; Teixeira, J.; Dragone, G. Mixotrophic cultivation of *Chlorella vulgaris* using industrial dairy waste as organic carbon source. *Bioresour. Technol.* **2012**, *118*, 61–66. [[CrossRef](#)]
43. Anjos, M.; Fernandes, B.D.; Vicente, A.A.; Teixeira, J.A.; Dragone, G. Optimization of CO₂ bio-mitigation by *Chlorella vulgaris*. *Bioresour. Technol.* **2013**, *139*, 149–154. [[CrossRef](#)] [[PubMed](#)]
44. Basu, S.; Roy, A.S.; Mohanty, K.; Ghoshal, A.K. Enhanced CO₂ sequestration by a novel microalga: *Scenedesmus obliquus* SA1 isolated from bio-diversity hotspot region of Assam, India. *Bioresour. Technol.* **2013**, *143*, 369–377. [[CrossRef](#)]
45. Tang, D.; Han, W.; Li, P.; Miao, X.; Zhong, J. CO₂ biofixation and fatty acid composition of *Scenedesmus obliquus* and *Chlorella pyrenoidosa* in response to different CO₂ levels. *Bioresour. Technol.* **2011**, *102*, 3071–3076. [[CrossRef](#)] [[PubMed](#)]
46. Mohsenpour, S.F.; Willoughby, N. Effect of CO₂ aeration on cultivation of microalgae in luminescent photobioreactors. *Biomass Bioenergy* **2016**, *85*, 168–177. [[CrossRef](#)]
47. Lichtenthaler, H.K.; Buschmann, C. Chlorophylls and carotenoids: Measurement and characterization by UV-VIS spectroscopy. *Curr. Protoc. Food Anal. Chem.* **2001**, *1*, F4.3.1–F4.3.8. [[CrossRef](#)]
48. Mecozzi, M. Estimation of total carbohydrate amount in environmental samples by the phenol-sulphuric acid method assisted by multivariate calibration. *Chemom. Intell. Lab. Syst.* **2005**, *79*, 84–90. [[CrossRef](#)]
49. Wang, H.; Nche-Fambo, F.A.; Yu, Z.; Chen, F. Using microalgal communities for high CO₂-tolerant strain selection. *Algal Res.* **2018**, *35*, 253–261. [[CrossRef](#)]
50. Dubois, M.; Gilles, K.A.; Hamilton, J.K.; Rebers, P.A.; Smith, F. Colorimetric method for determination of sugars and related substances. *Anal. Chem.* **1956**, *28*, 350–356. [[CrossRef](#)]
51. Varshney, P.; Beardall, J.; Bhattacharya, S.; Wangikar, P.P. Isolation and biochemical characterisation of two thermophilic green algal species- *Asterarcys quadricellulare* and *Chlorella sorokiniana*, which are tolerant to high levels of carbon dioxide and nitric oxide. *Algal Res.* **2018**, *30*, 28–37. [[CrossRef](#)]
52. Lowry, O.H.; Rosebrough, N.J.; Farr, A.L.; Randall, R.J. Protein measurement with the Folin phenol reagent. *J. Biol. Chem.* **1951**, *193*, 265–275. [[CrossRef](#)]
53. Varshney, P.; Sohoni, S.; Wangikar, P.P.; Beardall, J. Effect of high CO₂ concentrations on the growth and macromolecular composition of a heat- and high-light-tolerant microalga. *J. Appl. Phycol.* **2016**, *28*, 2631–2640. [[CrossRef](#)]
54. Bligh, E.G.; Dyer, W.J. A rapid method of total lipid extraction and purification. *Can. J. Biochem. Physiol.* **1959**, *37*, 911–917. [[CrossRef](#)] [[PubMed](#)]
55. Yadav, G.; Karemore, A.; Dash, S.K.; Sen, R. Performance evaluation of a green process for microalgal CO₂ sequestration in closed photobioreactor using flue gas generated in-situ. *Bioresour. Technol.* **2015**, *191*, 399–406. [[CrossRef](#)]
56. Kaiwan-Arporn, P.; Hai, P.D.; Thu, N.T.; Annachhatre, A.P. Cultivation of cyanobacteria for extraction of lipids. *Biomass Bioenergy* **2012**, *44*, 142–149. [[CrossRef](#)]
57. Wang, X.W.; Liang, J.R.; Luo, C.S.; Chen, C.P.; Gao, Y.H. Biomass, total lipid production, and fatty acid composition of the marine diatom *Chaetoceros muelleri* in response to different CO₂ levels. *Bioresour. Technol.* **2014**, *161*, 124–130. [[CrossRef](#)]
58. Widdel, F. Theory and measurement of bacterial growth. *MethodsX* **2019**, *6*, 2248–2257. [[CrossRef](#)]
59. Chae, S.R.; Hwang, E.J.; Shin, H.S. Single cell protein production of *Euglena gracilis* and carbon dioxide fixation in an innovative photo-bioreactor. *Bioresour. Technol.* **2006**, *97*, 322–329. [[CrossRef](#)] [[PubMed](#)]
60. Chiarini, A.; Quadrio, M. The light/dark cycle of microalgae in a thin-layer photobioreactor. *J. Appl. Phycol.* **2021**, *33*, 183–195. [[CrossRef](#)]
61. Xue, S.; Su, Z.; Cong, W. Growth of *Spirulina platensis* enhanced under intermittent illumination. *J. Biotechnol.* **2011**, *151*, 271–277. [[CrossRef](#)]
62. Toledo-Cervantes, A.; Morales, M.; Novelo, E.; Revah, S. Carbon dioxide fixation and lipid storage by *Scenedesmus obtusiusculus*. *Bioresour. Technol.* **2013**, *130*, 652–658. [[CrossRef](#)]
63. Chiang, C.L.; Lee, C.M.; Chen, P.C. Utilization of the cyanobacteria *Anabaena* sp. CH1 in biological carbon dioxide mitigation processes. *Bioresour. Technol.* **2011**, *102*, 5400–5405. [[CrossRef](#)]
64. Yang, Q.; Li, H.; Wang, D.; Zhang, X.; Guo, X.; Pu, S.; Guo, R.; Chen, J. Utilization of chemical wastewater for CO₂ emission reduction: Purified terephthalic acid (PTA) wastewater-mediated culture of microalgae for CO₂ bio-capture. *Appl. Energy* **2020**, *276*, 115502. [[CrossRef](#)]
65. Chinnasamy, S.; Ramakrishnan, B.; Bhatnagar, A.; Das, K.C. Biomass production potential of a wastewater alga *Chlorella vulgaris* ARC 1 under elevated levels of CO₂ and temperature. *Int. J. Mol. Sci.* **2009**, *10*, 518–532. [[CrossRef](#)] [[PubMed](#)]

66. Martínez, M.E.; Sánchez, S.; Jiménez, J.M.; El Yousfi, F.; Muñoz, L. Nitrogen and phosphorus removal from urban wastewater by the microalga *Scenedesmus obliquus*. *Bioresour. Technol.* **2000**, *73*, 263–272. [[CrossRef](#)]
67. Chiu, S.Y.; Kao, C.Y.; Chen, C.H.; Kuan, T.C.; Ong, S.C.; Lin, C.S. Reduction of CO₂ by a high-density culture of *Chlorella sp.* in a semicontinuous photobioreactor. *Bioresour. Technol.* **2008**, *99*, 3389–3396. [[CrossRef](#)]
68. Yen, H.W.; Ho, S.H.; Chen, C.Y.; Chang, J.S. CO₂, NO_x and SO_x removal from flue gas via microalgae cultivation: A critical review. *Biotechnol. J.* **2015**, *10*, 829–839. [[CrossRef](#)] [[PubMed](#)]
69. Ugwu, C.U.; Ogbonna, J.C.; Tanaka, H. Improvement of mass transfer characteristics and productivities of inclined tubular photobioreactors by installation of internal static mixers. *Appl. Microbiol. Biotechnol.* **2002**, *58*, 600–607. [[CrossRef](#)]
70. Sydney, E.; Sturm, W.; de Carvalho, J.; Soccol, V.T.; Larroche, C.; Pandey, A.; Soccol, C.R. Potential carbon dioxide fixation by industrially important microalgae. *Bioresour. Technol.* **2010**, *101*, 5892–5896. [[CrossRef](#)]
71. Kumar, K.; Banerjee, D.; Das, D. Carbon dioxide sequestration from industrial flue gas by *Chlorella sorokiniana*. *Bioresour. Technol.* **2014**, *152*, 225–233. [[CrossRef](#)] [[PubMed](#)]
72. Nayak, M.; Karemore, A.; Sen, R. Performance evaluation of microalgae for concomitant wastewater bioremediation, CO₂ biofixation and lipid biosynthesis for biodiesel application. *Algal Res.* **2016**, *16*, 216–223. [[CrossRef](#)]
73. Carlozzi, P. Dilution of solar radiation through “culture” lamination in photobioreactor rows facing south-north: A way to improve the efficiency of light utilization by cyanobacteria (*Arthrospira platensis*). *Biotechnol. Bioeng.* **2003**, *81*, 305–315. [[CrossRef](#)] [[PubMed](#)]
74. Hall, D.O.; Acien Fernández, F.G.; Guerrero, E.C.; Rao, K.K.; Grima, E.M. Outdoor helical tubular photobioreactors for microalgal production: Modeling of fluid-dynamics and mass transfer and assessment of biomass productivity. *Biotechnol. Bioeng.* **2003**, *82*, 62–73. [[CrossRef](#)] [[PubMed](#)]
75. López, M.G.-M.; Sanchez, E.D.R.; López, J.C.; Fernandez, F.G.A.; Sevilla, J.M.F.; Rivas, J.; Guerrero, M.; Grima, E.M. Comparative analysis of the outdoor culture of *Haematococcus pluvialis* in tubular and bubble column photobioreactors. *J. Biotechnol.* **2006**, *123*, 329–342. [[CrossRef](#)] [[PubMed](#)]
76. Kargupta, W.; Ganesh, A.; Mukherji, S. Estimation of carbon dioxide sequestration potential of microalgae grown in a batch photobioreactor. *Bioresour. Technol.* **2015**, *180*, 370–375. [[CrossRef](#)]
77. Ye, Q.; Cheng, J.; Guo, W.; Xu, J.; Li, K.; Zhou, J. Serial lantern-shaped draft tube enhanced flashing light effect for improving CO₂ fixation with microalgae in a gas-lift circumflux column photobioreactor. *Bioresour. Technol.* **2018**, *255*, 156–162. [[CrossRef](#)] [[PubMed](#)]